The Astrophysical Journal, 613:710–715, 2004 October 1

A SEARCH FOR TeV GAMMA-RAY EMISSION FROM HIGH-PEAKED FLAT-SPECTRUM RADIO QUASARS USING THE WHIPPLE AIR CERENKOV TELESCOPE

A. D. Falcone,[1,2] I. H. Bond,[3] P. J. Boyle,[4] S. M. Bradbury,[3] J. H. Buckley,[5] D. Carter-Lewis,[6] O. Celik,[7] W. Cui,[1] M. Daniel,[6] M. D'Vali,[3] I. de la Calle Perez,[3,8] C. Duke,[9] D. J. Fegan,[10] S. J. Fegan,[11] J. P. Finley,[1] L. F. Fortson,[4,12] J. Gaidos,[1] S. Gammell,[10] K. Gibbs,[11] G. H. Gillanders,[13] J. Grube,[3] J. Hall,[14] T. A. Hall,[15] D. Hanna,[16] A. M. Hillas,[3] J. Holder,[3] D. Horan,[11] A. Jarvis,[7] G. E. Kenny,[13] M. Kertzman,[17] D. Kieda,[14] J. Kildea,[16] J. Knapp,[3] K. Kosack,[5] H. Krawczynski,[5] F. Krennrich,[6] M. J. Lang,[13] S. LeBohec,[6] E. Linton,[4] J. Lloyd-Evans,[3] A. Milovanovic,[3] P. Moriarty,[18] D. Muller,[4] T. Nagai,[14] S. Nolan,[1] R. Ong,[7] R. Pallassini,[3] D. Petry,[19] F. Pizlo,[1] B. Power-Mooney,[10] J. Quinn,[10] M. Quinn,[18] K. Ragan,[16] P. Rebillot,[5] P. T. Reynolds,[20] H. J. Rose,[3] M. Schroedter,[11] G. Sembroski,[1] S. P. Swordy,[4] A. Syson,[3] K. Tyler,[1] V. V. Vassiliev,[7] S. P. Wakely,[4] G. Walker,[14] T. C. Weekes,[11] and J. Zweerink[7]

Received 2004 April 23; accepted 2004 June 5

ABSTRACT

Blazars have traditionally been separated into two broad categories based on their optical emission characteristics. Blazars with faint or no emission lines are referred to as BL Lacertae objects (BL Lacs), and blazars with prominent, broad emission lines are commonly referred to as flat-spectrum radio quasars (FSRQs). The spectral energy distribution of FSRQs has generally been thought of as being more akin to the low-peaked BL Lacs, which exhibit a peak in the infrared region of the spectrum, as opposed to high-peaked BL Lacs (HBLs), which exhibit a peak in UV/X-ray region of the spectrum. All blazars that are currently confirmed as sources of TeV emission fall into the HBL category. Recent surveys have found several FSRQs that exhibit spectral properties, particularly the synchrotron peak frequency, similar to HBLs. These objects are potential sources of TeV emission according to several models of blazar jet emission and the evolution of blazars. Measurements of TeV flux or flux upper limits could impact existing theories explaining the links between different blazar types and could have a significant impact on our understanding of the nature of objects that are capable of TeV emission. In particular, the presence (or absence) of TeV emission from FSRQs could confirm (or cast doubt on) recent evolutionary models that expect intermediate objects in a transitional state between FSRQ and BL Lac. The Whipple 10 m imaging air Cerenkov gamma-ray telescope is well suited for TeV gamma-ray observations. Using the Whipple telescope, we have taken data on a small selection of nearby ($z < 0.1$ in most cases) high-peaked FSRQs. Although one of the objects, B2 0321+33, showed marginal evidence of flaring, no significant emission was detected. The implications of this paucity of emission and the derived upper limits are discussed.

Subject headings: galaxies: active — gamma rays: observations — quasars: general

1. INTRODUCTION

Blazars, which exhibit the most extreme properties of all active galactic nuclei (AGNs), have traditionally been divided into two categories. These categories are separated from one another based on their optical line emission properties. BL Lac objects have either no emission lines or weak and narrow emission lines, with the typical definition requiring rest frame equivalent widths less than 5 Å (Stickel et al. 1991; Perlman et al. 1998), while flat-spectrum radio quasars (FSRQs) exhibit broad optical emission lines. Both classes of objects have extreme natures, characterized by a wide range of flux and spectral variability on many timescales. Objects from both classes also exhibit high levels of optical polarization.

The broadband radiation spectrum of blazars consists of two distinct components: a synchrotron spectrum component that spans radio to optical-ultraviolet wavelengths (and to X-rays for high-frequency peaked objects) and a high-energy component that can extend from the X-ray to the very high energy (VHE) gamma-ray (300 GeV $< E <$ 100 TeV) regime. Observationally, the spectra appear to have two distinct broad peaks when plotted in a νf_ν representation (Padovani & Giommi 1995; Fossati et al. 1998; Ghisellini et al. 1998). The emission in the first peak of the spectral energy distribution (SED) is generally considered to be synchrotron emission from relativistic electrons. The most widely invoked models that attempt to explain the higher energy emission of the second SED peak fall into the category of leptonic models. These leptonic models posit that the X-ray to gamma-ray emission is produced by inverse Compton scattering of lower energy

[1] Physics Department, Purdue University, West Lafayette, IN 47907.
[2] Current address: Whipple Observatory, Amado, AZ 85645.
[3] Department of Physics, University of Leeds, Leeds LS2 9JT, Yorkshire, England, UK.
[4] University of Chicago, Chicago, IL 60637.
[5] Department of Physics, Washington University, St. Louis, MO 63130.
[6] Department of Physics and Astronomy, Iowa State University, Ames, IA 50011.
[7] Department of Physics, UCLA, Los Angeles, CA 90095.
[8] Now at Department of Physics, Oxford University, UK.
[9] Physics Department, Grinnell College, Grinell, IA 50112.
[10] Physics Department, National University of Ireland, Belfield, Dublin 4, Ireland.
[11] Fred Lawrence Whipple Observatory, Harvard-Smithsonian Center for Astrophysics, Amado, AZ 85645.
[12] Astronomy Department, Adler Planetarium and Astronomy Museum, Chicago, IL 60637.
[13] National University of Ireland, Galway, Ireland.
[14] University of Utah, Salt Lake City, UT 84112.
[15] Department of Physics and Astronomy, University of Arkansas, Little Rock, AR 72204.
[16] Department of Physics, McGill University, Montreal, QC H3A 2T8, Canada.
[17] DePauw University, Greencastle, IN 46135.
[18] Galway-Mayo Institute of Technology, Galway, Ireland.
[19] NASA Goddard Space Flight Center, Code 661, Greenbelt, MD 20771.
[20] Department of Physics, Cork Institute of Technology, Cork, Ireland.

TABLE 1
CANDIDATE FSRQ SOURCE PROPERTIES

Source	z	R.A.	Decl.	$F_{\mathrm{X-ray}}$[a,b]	F_{radio} (mJy)[c]
B2 0321+33	0.062	03 24 41.1	+34 10 46	6.6[a]	368
PG 2209+184	0.070	22 11 53.8	+18 41 52	8.4[a]	116
WGA J0838+2453	0.028	08 38 11.1	+24 53 45	6.5[a]	32[d]
RGB J1413+436	0.090	14 13 43.7	+43 39 45	4.5[b]	50
RGB J1629+4008	0.272	16 29 01.3	+40 08 00	9.0[b]	20

NOTE.—Units of right ascension are hours, minutes, and seconds, and units of declination are degrees, arcminutes, and arcseconds.

[a] 0.3–3.5 keV flux (10^{-12} ergs cm^{-2} s^{-1}) corrected for galactic absorption taken from Perlman (2000).

[b] 0.1–2.4 keV flux (10^{-12} ergs cm^{-2} s^{-1}) uncorrected for galactic absorption taken from Perlman (2000) and Laurent-Muehleisen et al. (1998).

[c] 4.85 GHz radio flux taken from Gregory & Condon (1991).

[d] 4.85 GHz radio flux taken from Condon et al. (1995).

photons by beamed relativistic electrons. The low energy photon fields could arise from synchrotron continuum photons within the jet (e.g., Koenigl 1981), or they could arise from ambient photons from the accretion disk, which enter the jet directly (e.g., Dermer et al. 1992) or after scattering or reprocessing (e.g., Sikora et al. 1994). In addition to these leptonic models, hadronic models also attempt to explain the second component of the SED. These models involve proton-initiated cascades (e.g., Mannheim 1993) and/or proton synchrotron radiation (Muecke & Protheroe 2001; Aharonian 2000) as well as synchrotron emission from secondary muons and pions (Muecke et al. 2003).

In the blazar sequence proposed by Fossati et al. (1997) and Ghisellini et al. (1998), the first SED peak (the synchrotron peak) is at low energies for objects with a high bolometric luminosity, and the synchrotron peak is at high energies, sometimes in excess of 100 keV, for objects with low bolometric luminosity. In this sequence, FSRQs have their peaks at the lowest frequencies, and BL Lac objects have a first peak at higher frequencies. BL Lac objects are further divided into two categories: low-peaked BL Lacs (LBLs) exhibit a first peak at IR/optical frequencies, and high-peaked BL Lac objects (HBLs) exhibit a first peak at UV/X-ray frequencies.

With the advent of more recent deep X-ray and radio surveys, it is becoming clear that there exist objects that do not fall within the confines of this sequence. Some FSRQ objects that exhibit intermediate to high frequency spectral peaks, like their BL Lac cousins, are being discovered. Padovani et al. (1997) created a catalog based on early surveys and found that ~17% of the FSRQs in the sample had SEDs similar to HBLs, rather than LBLs. Perlman et al. (1998) and Landt et al. (2001) have found that ~30% of the FSRQs found in the DXRBS have X-ray to radio luminosity ratios characteristic of HBLs, while still retaining broad and luminous emission lines characteristic of FSRQs. The recent surveys attempt to bridge the gap between previous X-ray and radio selected objects, and they indicate the presence of a population of FSRQs with HBL-like SEDs, referred to as HFSRQs by Perlman et al. (1998). The possibility that these HFSRQs could produce GeV/TeV gamma-ray emission similar to their HBL cousins is explored in the observations described in this paper.

Although the catalog of confirmed and statistically significant (>5 σ) VHE gamma-ray sources now includes eight objects, six of which are AGNs, the only type of AGNs to be decisively detected at this time are HBLs (Weekes 2003; note that there are 18 VHE objects if one includes unconfirmed, yet published, sources). FSRQs with high frequency peaks offer an opportunity to expand the VHE gamma-ray catalog and simultaneously constrain the nature of HFSRQs as well as their associated emission mechanisms. By determining the categories of objects that can (and cannot) emit VHE gamma rays, the nature of the local medium required for such high energy acceleration can be characterized.

The remainder of this article is organized as follows. Section 2 identifies and describes the chosen HFSRQ objects that are candidate GeV/TeV gamma-ray sources. Section 3 describes the Whipple telescope and the observations performed with it. Section 4 presents the results of these observations, and § 5 discusses the implications of these results.

2. CANDIDATE SOURCE PROPERTIES

Candidate sources of TeV emission were chosen from lists of FSRQs based on several criteria, including spectral characteristics at radio to X-ray wavelengths, the location of the object in the sky, and the redshift of the object. The objects selected for observation are shown in Table 1. These candidates were selected from the source lists published by Perlman (2000) and Padovani et al. (2002) following the application of several selection criteria. Only objects with a high X-ray flux (>10^{-12} ergs cm^{-2} s^{-1} in the 0.1–2.4 keV energy band) were selected. Objects were also selected by looking at their radio to X-ray spectral energy distribution to look for signs of a particularly high frequency of the first SED peak when plotted in a νf_ν representation. The synchrotron peaks for the chosen candidates are in the range bounded by ~a few $\times 10^{14}$ Hz and $\sim 2 \times 10^{16}$ Hz. All of the sources chosen for this study have a high X-ray to radio luminosity ratio, as well as effective spectral indices that are more typical of HBLs than classical FSRQs. Another important requirement that was placed on the candidate sources was that they be easily observable by the Whipple Observatory, which is restricted to observations during clear and moonless nights of Northern Hemisphere sources.

The last restriction that was generally placed on the source candidate list was that they be nearby ($z < 0.1$). Sources at higher redshifts begin to have a significant fraction of their GeV/TeV emission absorbed due to pair production from the interaction of the high energy photon and infrared photons from the diffuse extragalactic background (Gould & Schreder 1967; Vassiliev 2000). At this time, the most distant confirmed source of TeV photons is at a redshift of $z = 0.129$ (H1426+428),

TABLE 2
IMAGE PARAMETERS USED FOR CHARACTERIZATION OF SHOWERS

Parameter	Description
Length	Length (major axis) of shower image
Width	Width (minor axis) of shower image
Distance	Distance from shower image centroid to camera center
Size	Sum of signals from all pixels in shower image
Max1	Largest signal recorded in any image pixel
Max2	Second largest signal recorded in any image pixel
α	Angle of shower major axis relative to line from camera center to image centroid

which places it at an optical depth of $\tau \approx 1$ for 400 GeV photons (de Jager & Stecker 2002; Horan et al. 2002). All of the candidate sources chosen for this study, with the exception of RGB J1629+401, are at redshifts less than $z = 0.1$. According to Padovani et al. (2002), RGB J1629+401 has an exceptionally high first peak in its SED ($\sim 2 \times 10^{16}$ Hz), so it was included in this survey, despite its redshift of $z = 0.272$.

3. OBSERVATIONS

Observations were performed throughout the 2001/2002 and 2002/2003 seasons at the Whipple Observatory, using the Whipple 10 m imaging air Cerenkov telescope (IACT).

3.1. *The Whipple* 10 m *Telescope and Data Analysis*

The Whipple telescope consists of a 10 m Davies-Cotton reflector (Davies & Cotton 1957) and a 490 pixel camera (Finley et al. 2001) composed of photomultiplier tubes (this analysis uses only the inner 379 pixels, which have 0.12° spacing). When a VHE gamma ray or cosmic ray hits the top of the atmosphere of the Earth, the resulting cascade of particles produces Cerenkov light as it propagates down through the atmosphere. This light is collected by the 10 m mirror, and the resulting image that is formed on the camera is used to characterize the shower. The parameters used for this characterization are: α, length, width, distance, size, max1, and max2 (Hillas et al. 1998; Punch et al. 1991). These parameters are described in Table 2, and the geometry of the parameters is shown in Figure 1. Because of different scattering angles during propagation of electromagnetic showers and hadronic showers, as well as the isotropic distribution of cosmic ray shower directions of origin, these characteristic parameters can be used to differentiate between gamma-ray and hadronic primary particles. By placing cuts on these parameters, the background due to the more numerous cosmic rays can be reduced, and thus the gamma-ray signal-to-noise ratio can be increased. These cuts are optimized each season by observing the Crab Nebula, which is a steady emitter of VHE gamma rays (Hillas et al. 1998), and maximizing the signal-to-noise ratio (significance). This procedure, of course, leads to a situation in which the analysis is optimized for a Crab-like spectrum. For sources that are significantly softer or harder, one has to be resigned to a loss in sensitivity, or one must reoptimize the cuts for a different spectral shape. The Crab is also used to calibrate the response of the instrument. The peak response of the telescope during the 2001/2002 and 2002/2003 seasons was at $\sim$400 GeV for a Crab-like spectrum.

The Whipple telescope is operated in two standard modes of operation. The first of these, referred to as the ON/OFF mode, requires that the 28 minute run in which the telescope is pointed at the candidate source (ON) be followed by another 28 minute run (OFF) in which the telescope is offset in right ascension by 30 minutes such that it images a region of sky through the same range of elevation and azimuth as the original source pointing. Since this OFF run is taken in nearly the same conditions as the ON run, without the candidate source in the field of view, it provides an independent measurement of the background. When operating in the other mode, referred to as TRACKING, one observes only at the sky coordinates of the source. This mode utilizes the large data set of OFF source observations taken throughout the season to estimate the background expected at small α-angles (where the source counts are expected for point-like sources), as a function of the background counts at large α-angles (where no source counts are expected). This procedure takes advantage of the fact that gamma-ray events from the source will preferentially produce an image with a small α-angle, while the more numerous background cosmic rays will be randomly oriented in the camera field of view. While this method allows more on-source data to be taken, it requires an accurate calculation of the tracking ratio, which is the ratio of events with α-angle between 20° and 65° to events with α-angle between 0° and 15° in the absence of a gamma-ray source. Since the analysis results are highly dependent on this tracking ratio, it must be calculated independently each season using OFF

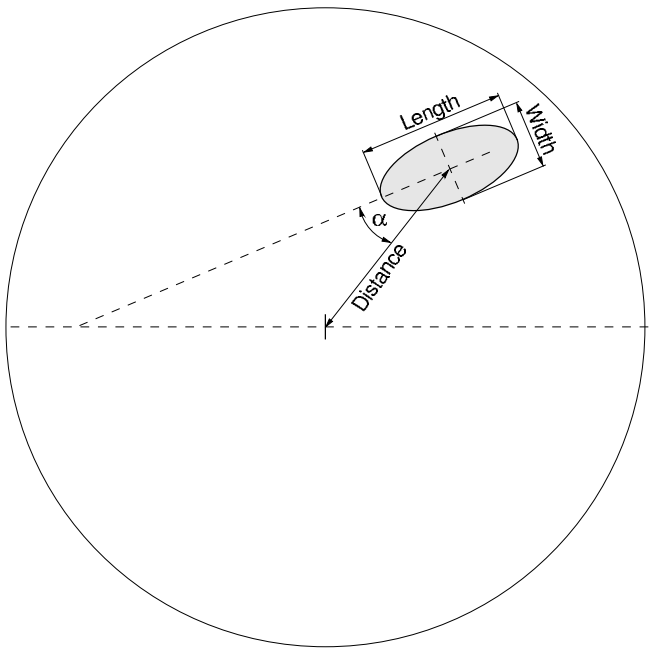

FIG. 1.—Image characterization of air showers imaged at the focal plane of the telescope. This cartoon shower projection has an elliptical shape that is typical of gamma ray– and cosmic ray–induced showers, and it has a large α-angle, which implies that the field of view is not centered on the source.

TABLE 3
WHIPPLE OBSERVATIONS OF CANDIDATE FSRQ SOURCES

Source (1)	$ON_{2001/2002}$ (minutes)[a] (2)	$ON_{2002/2003}$ (minutes)[a] (3)	σ[b] (4)	Upper Limit[c] (crab) (5)	Upper Limit[d] (10^{-11} ergs cm^{-2} s^{-1}) (6)	Upper Limit[e] (10^{-11} ergs cm^{-2} s^{-1}) (7)
B2 0321+33	320.3	331.5	1.56	0.10	0.52	0.68
PG 2209+184	217.6	0	0.15	0.13	0.71	0.97
WGA J0838+2453	0	781.6	0.15	0.05	0.29	0.32
RGB J1413+436	0	535.4	0.75	0.06	0.35	0.53
RGB J1629+4008	0	415.1	1.29	0.09	0.47	2.9

[a] ON refers to minutes spent on source during stable/clear weather conditions.
[b] Significance calculated as described in text.
[c] 95% confidence level upper limits calculated using method of Helene (1983), expressed as a fraction of the Crab flux ($R_{\rm Crab} = 2.84 \pm 0.16$ in 2001/2002 season and $R_{\rm Crab} = 2.55 \pm 0.13$ in 2002/2003 season).
[d] 95% confidence level upper limits for emission above $\sim$400 GeV, assuming a Crab-like spectrum as in Hillas et al. (1998); calculated using method of Helene (1983).
[e] 95% confidence level upper limits as described above, including the effect of absorption from the extragalactic background, using the baseline model of de Jager & Stecker (2002).

region data that have been taken when the telescope is operating in a state that is as close as possible to the state of operation when the TRACKING data are taken. This ratio has been calculated and applied to this analysis. For the 2001/2002 data the tracking ratio is 0.312 ± 0.003, and for the 2002/2003 data the tracking ratio is 0.3067 ± 0.0035.

Once the tracking ratio has been calculated using OFF source observations, the background for the ON source observations in the 0°–15° α-region, where all of the gamma-ray signal is expected, can be calculated. This is done by using the tracking ratio to scale the background events in the 20°–65° α-region to obtain the expected background counts in the 0°–15° α-region. After applying a simple propagation of error formula to this procedure, one obtains the significance

$$\sigma = \frac{N_{0^\circ-15^\circ} - r(N_{20^\circ-65^\circ})}{\sqrt{(N_{0^\circ-15^\circ}) + r^2 N_{20^\circ-65^\circ} + (\Delta r)^2 (N_{20^\circ-65^\circ})^2}}, \quad (1)$$

where $r \pm \Delta r$ is the tracking ratio and its associated statistical error. An important characteristic of this method for computing significance is that it incorporates the error on the tracking ratio, which is a quantity that is not accommodated by the method of Li & Ma (1983). It was found by Li & Ma (1983) that this type of significance calculation tends to be more conservative than their reported method of calculating significance. It should be noted that the error used to calculate this significance value is the statistical error; it does not include possible systematic errors.

A more detailed description of the standard analysis and the use of various cuts has been published previously in several articles including Mohanty et al. (1998), Reynolds et al. (1993), and Catanese et al. (1998).

3.2. *Source Observations*

Each of the candidate FSRQs was observed by the Whipple telescope, as shown in Table 3. Two of the candidates were observed during the 2001/2002 season (B2 0321+33 and PG 2209+184), and three additional candidates were observed during the 2002/2003 season (WGA J0838+2453, RGB J1413+436, and RGB J1629+4008). One source, B2 0321+33, was observed during both seasons since there was a marginal hint of flaring during the first season that merited a follow-up set of observations. During both seasons, the image parameter cuts were optimized independently, but the optimized cuts were identical for the two seasons, as expected for a stable camera configuration. Tracking ratios were calculated from a large number of OFF source runs taken during the relevant time frames. All of the observations reported here were taken at zenith angles less than 35°.

4. RESULTS

Significance values calculated using the method described above are shown in Table 3. None of the sources exhibited significant steady emission of gamma rays over the integrated time frame of the observations. Also shown in Table 3 are the 95% upper limit values for steady emission, calculated using the method of Helene (1983). Columns (5) and (6) of Table 3 are the upper limits for flux detected at Earth, and column (7) shows the upper limits for the flux at the source. This last column has been calculated using the optical depth of the extragalactic background for 400 GeV photons, as given by the baseline model of de Jager & Stecker (2002).

Although none of the FSRQs showed evidence for steady emission during the extended observations, one of them did exhibit marginal evidence of flaring during the 2001/2002 observing season. On 2001 October 22 (MJD 52204) two 28 minute observation runs were taken on B2 0321+33. The average gamma-ray rate of these two runs was 0.46 ± 0.14 times that of the Crab, which corresponds to a significance of 3.3 σ. The peak rate was 0.62 ± 0.19 crab. The light curve of data taken during that season is shown in Figure 2. If the trials factor is derived using the 16 observation nights of FSRQs during this season (combined for all sources), then the post-trials significance of this rate increase is 2.5 σ. While this rate increase was not significant enough to claim a detection of a variable source, it was enough to merit the further observations that were taken of this candidate in the 2002/2003 season.

5. DISCUSSION AND CONCLUSIONS

No significant emission has been detected from any of the candidate sources in this initial survey. There was marginal evidence of a rate increase observed in the B2 0321+33 light curve, but the statistical significance of this increase is 2.5 σ (post-trials significance), which could be accounted for by a statistical fluctuation. None of the other objects showed significant steady emission or any interesting features in their light curves.

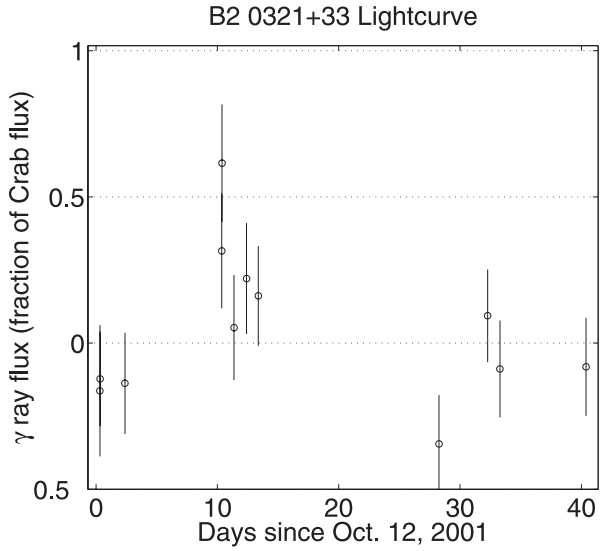

FIG. 2.—Light curve of B2 0321+33 using all data taken in the 2001/2002 observing season. Error bars are 1 σ statistical errors.

The upper limits presented here are the first VHE gamma-ray upper limits published for HFSRQs; however, they do not severely constrain the emission models because of the large amount of uncertainty in the models (and, of course, because of limited sensitivity of the telescope). Potential variability of the sources also leads to uncertainty in the expected flux. Typically, FSRQs and BL Lac objects are highly variable sources. Any VHE gamma-ray flux detected from these objects would most likely be from the sum of many flares or from a large flare that happened to be caught during the time frame of the observation. Applicable models of FSRQs have been made by Padovani et al. (2002). In this paper, several high-peaked and intermediate HFSRQs were modeled using a one-zone synchrotron inverse Compton model that was developed by Ghisellini et al. (2002). This model includes synchrotron self-Compton, as well as seed photon contributions from the disk and the broad-line region. The inclusion of the latter components may be important for these sources, which are known to have broad-line emission. While Perlman (2000) predicted that B2 0321+33, PG 2209+184, and RGB 1413+436 would be good TeV emission candidates, no modeling of the TeV flux was reported.

As a rough estimate of the expected flux, we have compared the SED of B2 0321+33 to those modeled by Padovani et al. (2002), and we find that it is similar to WGA J0546.6−6415, which has an estimated intrinsic VHE gamma-ray flux of $\sim 2 \times 10^{-12}$ ergs cm^{-2} s^{-1} above 400 GeV. This is below the value of our reported upper limit. With the exception of RGB J1629+4008, the VHE flux of the other objects is not as easy to predict within the context of published models. More modeling is necessary.

Padovani et al. (2002) directly modeled the SED of RGB J1629+4008, and they derived a synchrotron peak at 1.7×10^{16} Hz and a VHE gamma-ray flux of $\sim 2 \times 10^{-14}$ ergs cm^{-2} s^{-1} above 400 GeV. No mention was made of absorption of gamma rays by the diffuse IR background. This will produce a significant modification, since the source is at a large redshift of $z = 0.272$. Using the model of de Jager & Stecker (2002), this redshift corresponds to an optical depth of ~ 1.8 for 400 GeV gamma rays. The intrinsic source flux upper limit derived here is 0.29×10^{-12} ergs cm^{-2} s^{-1} above 400 GeV, which is certainly higher than the predicted source flux, so no strong constraints can be placed on the steady emission models for this object. The particularly high synchrotron peak and the potential for increased flux during flaring prompted these observations, but no variability was detected during the observations.

Cavaliere & D'Elia (2002) and Böttcher & Dermer (2002) posit that the blazar sequence (i.e., the relationship of blazar type and synchrotron peak location to the bolometric luminosity) is fundamentally dependent on the accretion rate $\dot{M}$. In this scenario, objects with large values of $\dot{M}$ are FSRQs and have large $L_{\rm bol}$ (more than $\sim 10^{46}$ ergs s^{-1}), while objects with small values of $\dot{M}$ are BL Lac objects and have small $L_{\rm bol}$ ($\sim 10^{44}$ ergs s^{-1}). Both of these models also predict an evolutionary scenario that progresses from FSRQs to BL Lacs, which leads to intermediate FSRQ objects that can have optical lines and large $L_{\rm bol}$, along with a synchrotron peak more like that of BL Lac objects. These objects should be excellent candidates for VHE gamma-ray emission. The fact that the observations presented here yield little or no VHE emission does not support this scenario, but these observations certainly do not rule out the proposed models for two reasons. It is possible that these intermediate objects have optical depths that are large enough to prevent the escape of VHE emission. It is also possible that the handful of objects in this initial survey were not in a high flaring state at the time of observation. The inherent variability of blazars makes the detection of both BL Lac and FSRQ VHE emission difficult, as evidenced by the paucity of detected sources relative to the number of observed BL Lac candidates in past campaigns (de la Calle Pérez et al. 2003; Horan et al. 2004). More observations of these and other objects will be necessary.

Although no detection of VHE gamma-ray emission has been reported from this initial survey, dim or variable emission from these candidates, or emission from other similar candidates, is not ruled out. This work should be continued with more sensitive instruments, such as the next generation of IACTs (VERITAS, HESS, MAGIC, and CANGAROO-III) that are beginning to come on line at the time of this writing (Krennrich et al. 2004; Hinton et al. 2004; Lorenz et al. 2004; Kubo et al. 2004). More modeling of these objects is required in order to predict the high-energy flux more accurately, and therefore, the potential of a given HFSRQ to be a gamma-ray source. In addition, the continued progress of deeper X-ray to gamma-ray surveys (*Swift*, *EXIST*, *INTEGRAL*, *GLAST*) and X-ray imaging (*Chandra*, *XMM-Newton*) may reveal additional TeV FSRQ candidates with higher frequency peaks in the SED and/or increased high-energy flux potential.

We acknowledge the technical assistance of E. Roache and J. Melnick. This research is supported by grants from the US Department of Energy, Enterprise Ireland, and PPARC in the UK.

REFERENCES

Aharonian, F. A. 2000, NewA, 5, 377
Böttcher, M., & Dermer, C. D. 2002, ApJ, 564, 86
Catanese, M., et al. 1998, ApJ, 501, 616
Cavaliere, A., & D'Elia, V. 2002, ApJ, 571, 226
Condon, J. J., Anderson, E., & Broderick, J. J. 1995, AJ, 109, 2318
Davies, J. M., & Cotton, E. S. 1957, J. Solar Energy, 1, 16
de Jager, O. C., & Stecker, F. W. 2002, ApJ, 566, 738
de la Calle Pérez, I., et al. 2003, ApJ, 599, 909
Dermer, C. D., Schlickeiser, R., & Mastichiadis, A. 1992, A&A, 256, L27
Finley, J. P., et al. 2001, in Proc. 27th Int. Cosmic Ray Conf. (Hamburg), 199
Fossati, G., Celotti, A., Ghisellini, G., & Maraschi, L. 1997, MNRAS, 289, 136
Fossati, G., et al. 1998, MNRAS, 299, 433

Ghisellini, G., Celotti, A., & Costamante, L. 2002, A&A, 386, 833
Ghisellini, G., et al. 1998, MNRAS, 301, 451
Gould, R. P., & Schreder, G. P. 1967, Phys. Rev., 155, 1408
Gregory, P. C., & Condon, J. J. 1991, ApJS, 75, 1011
Helene, O. 1983, Nucl. Instrum. Methods Phys. Res., 212, 319
Hillas, A. M., et al. 1998, ApJ, 503, 744
Hinton, J., et al. 2004, NewA Rev., 48, 331
Horan, D., et al. 2002, ApJ, 571, 753
———. 2004, ApJ, 603, 51
Koenigl, A. 1981, ApJ, 243, 700
Krennrich, F., et al. 2004, NewA Rev., 48, 345
Kubo, H., et al. 2004, NewA Rev., 48, 323
Landt, H., Padovani, P., Perlman, E. S., Giommi, P., Bignall, H., & Tzioumis, A. 2001, MNRAS, 323, 757
Laurent-Muehleisen, S. A., Kollgaard, R. I., Ciardullo, R., Feigelson, E. D., Brinkmann, W., & Siebert, J. 1998, ApJS, 118, 127
Li, T., & Ma, Y. 1983, ApJ, 272, 317
Lorenz, E., et al. 2004, NewA Rev., 48, 339
Mannheim, K. 1993, A&A, 269, 67
Mohanty, G., et al. 1998, Astropart. Phys., 9, 15
Muecke, A., & Protheroe, R. J. 2001, Astropart. Phys., 15, 121
Muecke, A., Protheroe, R. J., Engel, R., Rachen, J. P., & Stanev, T. 2003, Astropart. Phys., 18, 593
Padovani, P., Costamante, L., Ghisellini, G., Giommi, P., & Perlman, E. 2002, ApJ, 581, 895
Padovani, P., & Giommi, P. 1995, ApJ, 444, 567
Padovani, P., Giommi, P., & Fiore, F. 1997, Mem. Soc. Astron. Italiana, 68, 147
Perlman, E. S. 2000, in AIP Conf. Proc. 515, GeV-TeV Gamma Ray Astrophysics Workshop, ed. B. L. Dingus, M. H. Salamon, & D. B. Kieda (New York: AIP), 53
Perlman, E. S., Padovani, P., Giommi, P., Sambruna, R., Jones, L. R., Tzioumis, A., & Reynolds, J. 1998, AJ, 115, 1253
Punch, M., et al. 1991, in Proc. 22nd Int. Cosmic Ray Conf. (Dublin), 1, 464
Reynolds, P., et al. 1993, ApJ, 404, 206
Sikora, M., Begelman, M. C., & Rees, M. J. 1994, ApJ, 421, 153
Stickel, M., Padovani, P., Urry, C. M., Fried, J. W., & Khür, H. 1991, ApJ, 374, 431
Vassiliev, V. V. 2000, Astropart. Phys., 12, 217
Weekes, T. C. 2003, in Proc. 28th Int. Cosmic Ray Conf. (Tsukuba), 8, in press